Journal of Constructional Steel Research 229 (2025) 109492

Contents lists available at ScienceDirect

Journal of Constructional Steel Research

journal homepage: www.elsevier.com/locate/jcsr

Behaviour and design resistance of long bolts in tension

Neda Janković [a,*], Filip Ljubinković [a], Jorge Conde [b], Jordi Costa [c], Luís Simões da Silva [a,1]

[a] University of Coimbra, ISISE, ARISE, Department of Civil Engineering, Portugal
[b] Universidad Politécnica de Madrid, Departamento de Física y Estructuras de Edificación, Av. Juan de Herrera, 4, 28040 Madrid, Spain
[c] Tornillería Industrial, S.A. c/ Catalunya 11, P.I. Can Oller, 08130 Santa Perpetua de Mogoda, Barcelona, Spain

ARTICLE INFO

Keywords:
Long bolts
Bi-directional bolts
Design tensile resistance
Stiffness
Ductility
Eurocode

ABSTRACT

Long bolts, also known as bi-directional bolts, have multiple applications in structural engineering, particularly as an instrumental part of the adaptability and reusability of steel members. Despite that, the long bolt design is not properly covered by current standards. This paper describes an experimental and analytical study to characterize the long bolts in tension for their inclusion in the component method precluded by Eurocode 3. The study is part of a wider campaign (including the behaviour in shear, preloading, and relaxation of the bolts) developed in the framework of the European Research Project CONNECT4C. The study shows that the current design expressions for bolt resistance and stiffness can be used for long bolts in tension, regardless of bolt material or finishing surface. A bolt material model is proposed for possible inclusion in steel design standards. Finally, it is also recommended to adopt double nuts in long bolts to avoid premature thread stripping.

1. Introduction

In many structural systems, long steel bolts may be advantageous. They allow the connection of parts that may not be in contact and are increasingly used in demountable solutions, potentially leading to improved adaptability and reusability in construction. Several innovative applications have profited from the deformability of long bolts, such as self-centring structural solutions [1,2]. They provide an excellent fastening solution whenever the grip length exceeds the available lengths for standard structural bolts, for instance, the connection across concrete-filled tubes (Fig. 1(a)), joints connecting very thick plates (Fig. 1(b)), foundation anchors (Fig. 1(c)).

In the context of this paper, "long bolts" are defined as structural bolts that are manufactured from circular steel rods instead of a steel coil and are not subjected to heat treatment, in contrast to standard structural bolts. This type of threaded rods with metric threads is covered by EN 15048 [4], where they are referred to as "stud bolts". They are needed whenever a bolt head is undesirable or longer lengths are required because standard structural bolts are usually available with maximum lengths (e.g. standard structural bolts according to EN 14399–4 [5] are specified in this standard with maximum lengths that may vary from 95 mm for an M12 diameter bolt up to 200 mm for an M36 diameter bolt, although it may be possible to order them with longer lengths). Hence, the behaviour of long bolts may differ from standard structural bolts although their design properties must comply with EN 1993–1-8 [6].

The ongoing RFCS CONNECT4C European Project [7] is focused on developing demountable and adaptable structural solutions that promote the reuse of reclaimed steel members. A key aspect of the project relates to the development of innovative joints that provide very large tolerances to accommodate reclaimed steel members without the need to cut or extend them [8]. These joints comprise the extensive use of long bolts that are dominantly subject to pure tension with or without shear. However, long bolts are not well covered in the literature and are not clearly supported by specific product standards.

To fill this knowledge gap, this paper aims to verify and characterize their behaviour in tension and assess whether the design expressions for tension resistance and stiffness in EN 1993–1-8 [6], calibrated for standard structural bolt assemblies, can be applied to long bolts. To this end, an experimental campaign of long bolts in tension is reported. Secondly, a material law is proposed for the steel bolt material. Finally, the applicability of the design expressions in EN 1993–1-8 [6] is performed and a reliability assessment is carried out to validate the choice of the partial factor γ^{*}_{M2}, in line with the target reliability index of EN 1990, Annex D [9].

* Corresponding author.
E-mail address: neda.jankovic@uc.pt (N. Janković).
[1] The author Luís Simões da Silva is an editor of this journal. In accordance with policy, Luís Simões da Silva was blinded to the entire peer review process.

https://doi.org/10.1016/j.jcsr.2025.109492
Received 29 December 2024; Received in revised form 20 February 2025; Accepted 3 March 2025
Available online 10 March 2025

Symbols and acronyms

Acronyms

B	Black surface of the long bolt
BF	Bolt fracture failure mode
G	Galvanized surface of the long bolt
FT	Fully threaded bolts
LC	Load cell
LVDT	Linear velocity displacement transducers
N1	Single nut configuration for long bolt
N2	Double nut configuration for long bolt
PT	Partially threaded bolts
TS	Thread stripping failure mode

Latin letters

A	Gross cross-section area, Percentage of elongation after fracture
A_{gt}	Elongation percentage corresponding to the tensile strength
A_f	Elongation after fracture for full-size fasteners
A_s	Tensile area of bolt
d	External diameter of the fully threaded bolt
d_s	Diameter of the unthreaded shank
d_1	Basic minor diameter of bolt threads
d_2	Basic pitch diameter of the bolt thread
d_3	Minor diameter of the bolt thread
E	Young's modulus of steel
F	Force, load
$F_{t,Rd}$	Design tension resistance of bolt
f_{yb}	Bolt yield strength
f_{ub}	Bolt tensile strength
H	Height of the fundamental triangle of the thread
k_2	Adjustment factor for tension resistance of bolt
l_{15}	Bolt length corresponding to 15 threads
L	Total bolt length
L_b	Bolt elongation length
L_g	Grip length
$L_{g,N1}$	Operational grip length for tests with single nuts
$L_{g,N2}$	Operational grip length for tests with double nuts
L_t	Distance between the nut face and the end of the threaded part (runout)
L_{tl}	Thread engagement length
P	Thread pitch
R_p	Stress at 0.2 % non-proportional elongation
R_m	Tensile strength
R_f	Stress at fracture point
$r_{t,nom,i}$	Design resistance function (nominal properties)
t_n	Thickness of nut
t_w	Thickness of washer
u	Elongation of the bolt

Greek letters

ε_{sh}	Strain hardening strain
ε_u	Ultimate strain
γ_{M2}	Partial factor

2. Background

2.1. Geometry and normative framework

In Europe, standard structural bolts must comply with product standards (EN 15048 [4] for non-preloaded structural bolting assemblies and EN 14399 [10] for high-strength structural bolting assemblies for preloading) and are supplied as an assembly that comprises the bolt, the nuts and the washers (the latter part of the assembly in case of EN 15048). These product standards refer to additional ISO standards that specify mechanical properties [11], dimensional properties [12–18], dimensional tolerances [19,20], coating systems and surface properties [21–23] and inspection procedures [24–26], as summarized in Table 1 [27].

Concerning high-strength structural bolting assemblies for preloading, two different systems are available, HR (EN 14399–3 [28]) and HV bolts (and EN 14399–4 [5]), which mainly differ in their failure mode under pure tensile force, particularly in terms of both residual strength

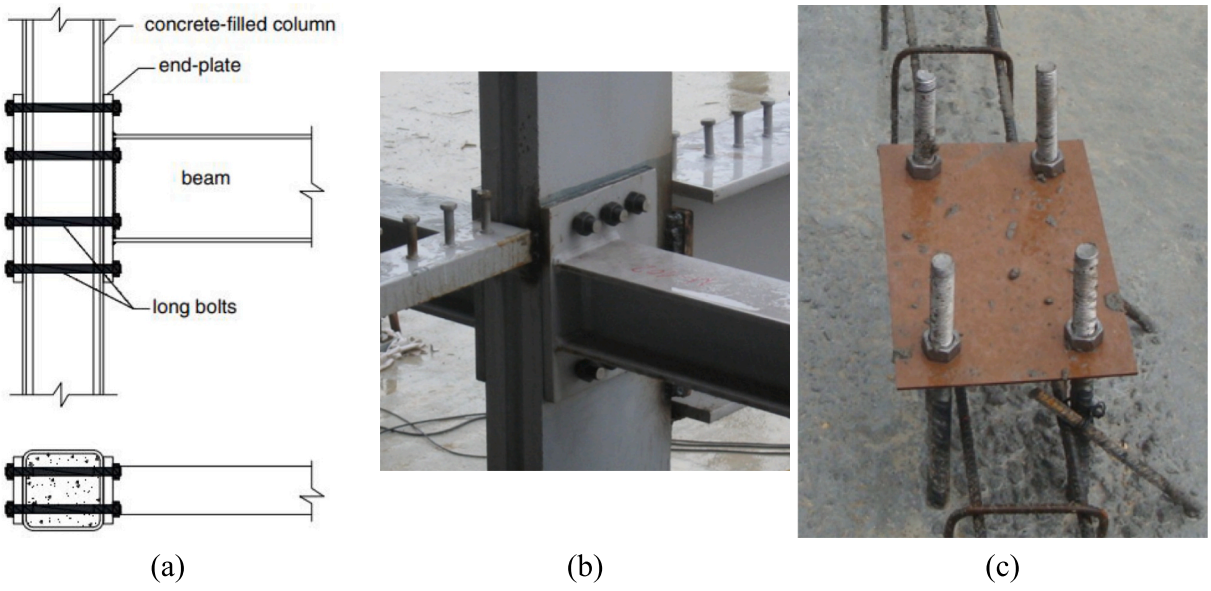

Fig. 1. Applications of long bolts: (a) Concrete-filled tubes [3]; (b) Joint with large grip length (Centro de Arte y Tecnología, Segovia, Spain. Picture by the authors); (c) Foundation anchor (Bodega BRVS, La Rioja, Spain. Picture by the authors).

Table 1
Summary of standards for structural bolts.

	Product standard	Symbology and general requirements	Mechanical properties (bolts, nuts, washers)	Dimensional properties	Dimensional tolerances	Coating systems	Inspection
Non-preloaded bolt assemblies in carbon steel and alloy steel	EN 15048	ISO 225	ISO 898	ISO 261 ISO 724 ISO 888	ISO 965	ISO 4042	EN 15048–2 ISO 3269
High-strength bolting assemblies for preloading	EN 14399	ISO 8992		ISO 3508 ISO 4014 ISO 4017 ISO 4753	ISO 4759-1	ISO 6157 ISO 10683	ISO 14399-2 ISO 3269

and deformation capacity at the point of collapse. The HR type assemblies achieve ductility primarily through the plastic elongation of the bolt, while the HV type assemblies attain ductility through the plastic deformation of the engaged threads [10]. Hence, the first type is characterized by a necking fracture in the threaded part of the bolt, while the second usually fails by nut stripping, without shank necking [29].

Fig. 2 illustrates the geometry of a typical fully threaded (FT) and partially threaded (PT) structural bolt assembly. It is composed of a bolt and a nut, with or without washers depending on the type of bolt (non-preloaded or preloaded) and the joint material. In Fig. 2(a), the distance between the inner faces of two washers, denoted as L_g, represents the grip length, i.e. the thickness of the parts being fastened, whereas the distance between the nut face and the end of the threaded part (runout) is denoted by L_t. L, L_b and L_{tl} represent the total bolt length, the bolt elongation length (defined as the grip length + washer thicknesses + half the combined height of the bolt head and the nut) and thread engagement length (defined as the axial distance over which the internal and external threads of a fastener overlap, ensuring the distribution of load), respectively.

A is the cross-section area of the shank while A_s denotes the cross-section area of the threaded length, given by Eqs. (1a) and (1b) according to ISO 898-1 [11].

$$A = \frac{\pi}{4} d_s^2 \tag{1a}$$

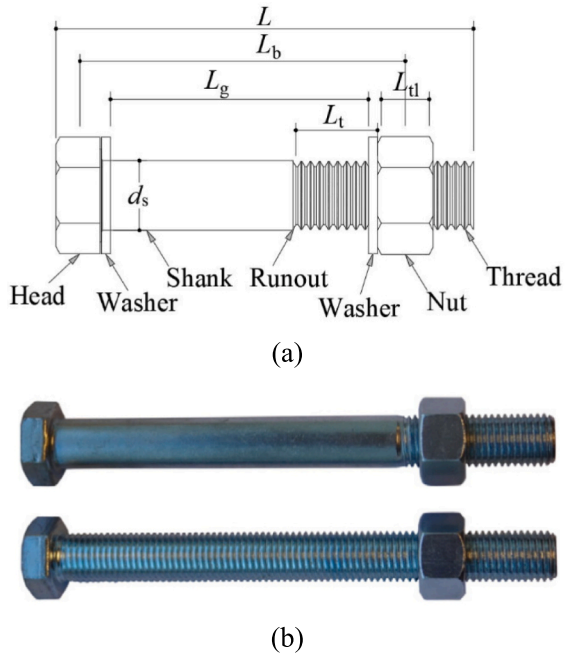

Fig. 2. Geometry of a standard structural bolt: (a) Lengths definition; (b) Partially and fully threaded specimens [30].

$$A_s = \frac{\pi}{4}\left(\frac{d_2 + d_3}{2}\right)^2 \tag{1b}$$

where d_s is the diameter of the shank, d_2 is the basic pitch diameter of the bolt thread, and d_3 is the minor diameter of the bolt thread. These and other relevant parameters (d_1 - the basic minor diameter of bolt threads, P - thread pitch and H - the height of the fundamental triangle of the thread) are explained in standards ISO 724 [13], and ISO 68-1 [31].

Fig. 3 illustrates the geometry of a long bolt assembled with single nuts. Unlike standard hexagonal head structural bolts, it does not exhibit a bolt head because of the manufacturing process, so nuts are required at both ends. In this study, long bolts are fully threaded rods, although they can also be manufactured as partially threaded. The total length of the bolt, denoted as L, is only limited by the length of the rod. Additionally, L_b refers to the bolt elongation length, L_g is the grip length, L_{tl} is the thread engagement length, and d is the external diameter of the bolt.

2.2. Behaviour of bolts in tension

2.2.1. Standard structural bolts

Fig. 4 depicts an example of the force-elongation curve of a bolt tested in tension. In the initial part, the curve exhibits a linear elastic behaviour, followed by the development of plastic deformation with a progressive reduction of stiffness (k_b) until the failure of the bolt. It is noted that the resistance of carbon steel bolts loaded in tension is dictated by the threaded part since it is the weakest part, with the minimum cross-section area, approximately given by $A_s/A = 0.78$ [32].

The behaviour of standard structural bolts in tension has been studied by many authors for many years. Recently, Stranghöner et al. [32] reassessed the resistance of carbon steel bolts subject to tension, shear, and combined forces. Besides carrying out a large test campaign, the authors collected the available experimental results in the literature and concluded that the design expressions in EN 1993–1-8 [6] could be improved while still satisfying the target probability of failure of the EN 1990, Annex D [9].

It is well known (Kulak et al. [33]) that the bolt tensile resistance depends on the way the tension is applied. Tightening the nut introduces torsional stresses and more complex combined tension-torsional stress condition in the bolt. Torquing a bolt until failure results in a reduction of both the ultimate load and the ultimate deformation as compared with the corresponding values determined from a direct tension test. Additionally, in the case of subsequently loading the bolt in direct tension after it has already been loaded by tightening the nut, there is not a significant drop in ultimate strength. This is relevant for the requirements for preloaded and non-preloaded bolts and justifies the need for two distinct product standards [4,10].

Two distinct failure modes are observed in bolts subjected to tension: (i) bolt fracture, and (ii) thread stripping (nut or bolt). Grimsmo et al. [30] studied the influence of the length L_t (see Fig. 2), on the bolt failure mode. They concluded that the probability of the thread failure can be reduced by increasing this length. In addition, the authors simulated the influence of high nuts, designed according to ISO 4033: Hexagon high

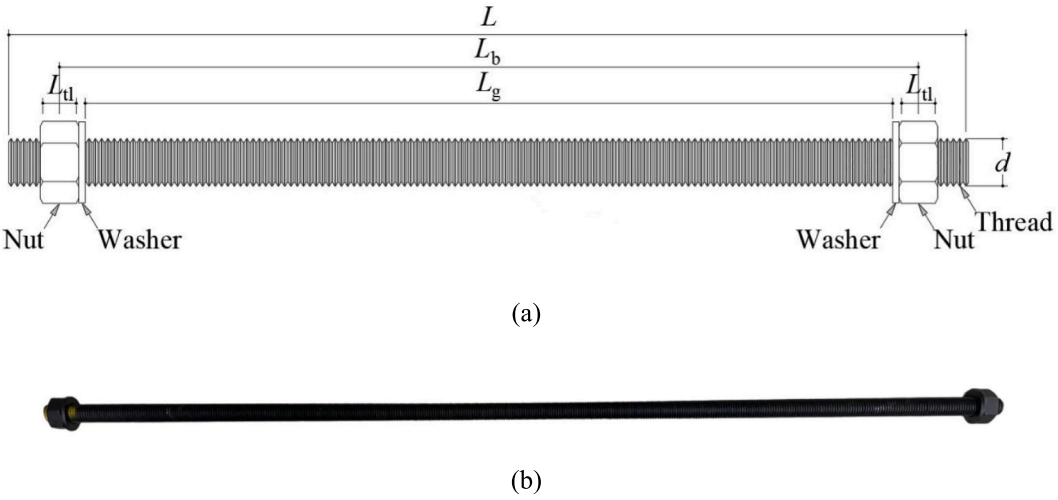

Fig. 3. Geometry of a structural long bolt: (a) Geometrical definition; (b) Example of M20 1000 mm long bolt.

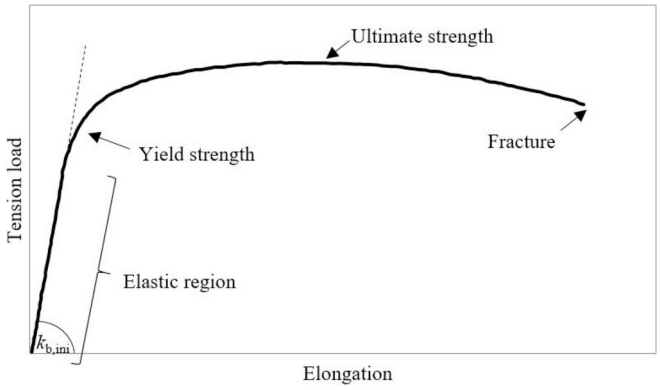

Fig. 4. Points of interest on the force-elongation curve of a standard bolt subjected to tensile force.

nut [34]. The nut height had a major impact on the results since the bolt showed a more ductile behaviour than with a regular nut, switching the failure mode from thread stripping to bolt fracture. Similarly, Alexander [35] claims that as the number of threads is reduced, the failure mode changes from bolt fracture to stripping. Consequently, by increasing the nut height, the probability of thread stripping decreases, and the probability of bolt fracture increases. Tartaglia et al. [36] confirmed that nut stripping failure is more characteristic of HV bolts, while HR bolts usually fail by bolt fracture, according to their design (EN 14399–1 [10]). Despite experiencing different failure modes, both bolt types showed similar evaluation of forces in the performed tests. The influence of the use of double nuts was experimentally studied by Grimsmo et al. [37], showing that it prevented thread stripping.

Concerning the influence of fully threaded vs partially threaded bolts, Yang et al. [38] numerically studied the fracture behaviour of the PT and FT bolts under tensile loading. PT bolts show higher yield and ultimate strengths, but smaller deformation capacity compared to FT bolts, confirming earlier results by Grimsmo et al. [30].

Hu et al. [39] studied the influence of surface finishing on failure by thread stripping. They concluded that the nuts with zinc plating surface led to the thread stripping failure due to the threads of the nuts being over-tapped (by 0.4 mm) for the coating process. They propose the use of nuts one material property class higher than the bolts to decrease the probability of failure by nut stripping.

2.2.2. Long bolts

Unlike conventional bolts, long bolts are not very well covered in the literature. Most references deal with long bolts as a part of a bolted end-plate beam to concrete-filled hollow section column connections [3,40,41]. In this case, long bolts are subject mainly to shear and are not relevant for this paper.

Fransplass et al. [42–44] studied long bolts manufactured from threaded rods subject to tension and combined tension and shear at low and elevated strain rates. The tests were carried out using a purpose-made fixture and by fixing this element in different positions various grip lengths were studied, in the range of 0.41 mm to 9.8 mm. It was concluded that the number of threads in the grip length influenced the failure of the bolt. In most cases, the failure mode was by bolt fracture, but bolts with shorter grip lengths showed significantly lower ductility compared to the ones with longer grip lengths. Additionally, based on the analytical models developed by Alexander [35], they propose modified equations for the prediction of the thread stripping resistance [42]. However, since they tested small grip lengths and small diameter rods in mild steel, M5 class 4.6, the validity of their conclusions for the present study may be limited.

Finally, Loureiro et al. [45] carried out an initial study aiming at assessing the influence of using long threaded structural bolts in unequal-depth internal node steel joints instead of standard structural bolts. Threaded bars were used in the tensile and compression parts of the connection. They concluded that the threaded bolt joints led to an increase in resistance and rigidity of 59 % and 24.5 %, respectively.

2.3. Manufacturing of long bolts

The production of standard structural bolts follows four steps: i) selection of the steel coil based on chemical composition, ii) stamping process (usually cold forging), to shape the head geometry and production of the thread by means of threading dies; iii) heat treatment (annealing + tempering), by furnace or induction, to obtain the desired mechanical properties; iv) durability coating. The production of long bolts presents some differences when compared to standard structural bolts, namely: i) they are not manufactured from steel coil but from a long calibrated rod (usually 6 m long); ii) they are not subjected to head-shaping cold forging, only to threading; iii) they are not subjected to heat treatment process; iv) after production, the bar is cut to the desired measure (usually 1 m pieces) and the cut ends are chamfered. If subjected to heat treatment, the long bolt recovers the initial curvature of the rod, thus requiring a subsequent straightening process which is complex and uneconomical.

2.4. Design expressions

Stranghöner et al. [32] provide a review of the design expressions for the resistance of carbon steel bolts in EN 1993–1-8, AISC 360–22 [46] and AS4100 [47] codes. Table 2 summarizes the design expressions for resistance and stiffness of bolts in tension in EN 1993–1-8 [6]. L_b is the bolt elongation length, measured from nut centre to head centre or midpoints between two nuts (in case double nuts are used), see Fig. 2 and Fig. 3. Eq. (3) is applied for a single bolt and hence, considers half the stiffness value of the component "Bolt in Tension" given in EN 1993–1-8 [6] (which is defined for a single bolt-row comprising two bolts).

3. Experimental programme

3.1. Definition of the test program

The main objective of the first experimental campaign within the CONNECT4C research project [7] is to characterize the behaviour of long bolts in tension, by extracting *F-u* curves (where *F* is the applied tensile force and *u* is the elongation of the bolt, see Fig. 5), and comparing the obtained results of tensile resistance and initial stiffness with Eqs. (2) and (3).

A total of 66 tensile tests were performed, covering the following parameters:

- Bolt diameter (M20, M24, M27 and M30),
- Bolt class (8.8 and 10.9),
- Surface finishing (B – black and G – galvanized),
- Number of nuts provided on each bolt end (N1 – single and N2 – double nut).

Each test was labelled concatenating the letter 'T' (for tension) with the specifications for its defining parameters. As an example, 'T25-M24–10.9-B-N1' corresponds to a tension test (T), order of test in the series total (25th), long bolt diameter M24 class 10.9, with black (B) surface finishing, and a single nut (N1) on each bolt end. This labelling system is used hereinafter. A summary of all tests is given in Table 3. Three repetitions were performed for each set of parameters to capture variability.

Double-nut tests (N2) were initially planned only for bolts M20 and M27. After initial testing, it was observed that most bolts with a single nut (N1) experienced nut stripping failure. Since this is an undesirable failure mode [30], additional double-nut tests were performed for M24 and M30 bolts, except for M24 8.8 bolts, where failure by bolt fracture was observed in all single-nut tests (N1). These additional tests are indicated with parenthesis in Table 3.

Table 2
Design specifications for bolts in tension in EC3–1-8:2005 and EC3–1-8:2024.

Tension resistance		(2)
Fully and partially threaded bolts	$F_{t,Rd} = \frac{k_2 f_{ub} A_s}{\gamma_{M2}}$	
Initial stiffness		(3)
Non-preloaded bolts	$k_b = \frac{0.8EA_s}{L_b}$	
Preloaded bolts	∞	

k_2: reduction factor with $k_2 = 0.9$ (exception: for countersunk bolts $k_2 = 0.63$); in EN 1993–1-8:2024, the value of 0.9 (or 0.63) are given directly | f_{ub}: nominal tensile strength of the bolt | A_s: tensile stress area of the bolt | γ_{M2}: partial factor ($\gamma_{M2} = 1.25$) | E: Young's Modulus of the bolt material | L_b: the bolt elongation length.

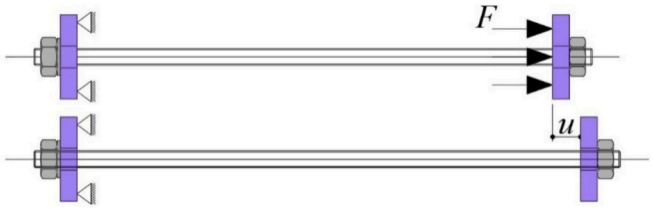

Fig. 5. Tensile force application.

Table 3
Summary of the performed tests.

Bolt diameter	Class	Surface	No. of nuts on each side	Repetitions	No. of tests
M20	8.8 and 10.9	B and G	N1, N2	3	24
M24	8.8	B and G	N1	3	6
M24	10.9	B and G	N1 (+N2)	3	6 (+6)
M27	10.9	B and G	N1, N2	3	12
M30	10.9	B and G	N1 (+N2)	3	6 (+6)
				Total	**66**

3.2. Experimental setup

The experimental setup is depicted in Fig. 6, with the relevant parts numbered in Fig. 6(b) and some additional pictures shown in Fig. 7. The test setup comprises a reaction frame (6) formed by vertical columns and a horizontal strong beam supporting a 6 MN jack. The jack piston was screwed to a pinned part (10) transferring load and displacement to a plate (9) bolted to the top beam (2), which was supported by a guiding system (4), sliding on the reaction frame columns (6) with the interposition of Teflon pads to minimize friction. A bolted connection tool (3) joined the top beam (2) to the long bolt specimen. The tool had a 36 mm diameter hole, and therefore an adjustment washer (5) was needed according to the long bolt diameter to provide conventional hole tolerance. The same connecting tool (3, 5) placed upside-down was used to fix the specimen to the bottom beam (1), whose vertical motion was prevented by two brackets (7) attached to the reaction frame columns (6), with load cells (8) interposed to measure the vertical reactions. The bottom beam (1) was supported by the same system as the top one (4, 6). When the jack piston moved upward, the top beam (2) moved with it, stretching the bolt which was fixed at the bottom beam (1).

The total bolt length *L* (see Fig. 3) was constant for all tests, 1000 mm. Table 4 lists the geometry and resistance of all bolts, as well as the operational grip lengths $L_{g,N1}$ (single nut N1) or $L_{g,N2}$ (double nut N2), calculated according to the details of the bolt assembly, including washers, nuts, and the protruding threaded portion of the bolt beyond the nuts (approximately 5 threads, as shown in Fig. 7(c)).

3.3. Test procedure and instrumentation

The test was performed by applying a displacement to the top retaining beam, by means of a 6 MN hydraulic jack (see Fig. 7(b)) attached to the beam with a pin connection. The test speed was 0.025 mm/s. During the tests, the following data was acquired (see Fig. 8):

- Applied force and reactions, using load cells (LCs),
- Displacements, using LVDTs (Linear velocity displacement transducers).

Two load cells with capacities of 2 MN were used for load measurements. They were labelled as LC-1 and LC-2 and positioned between the lower retaining beam and the reaction brackets, as shown in Fig. 8(a) and (c).

In total, 12 LVDTs were used for measuring vertical absolute (label

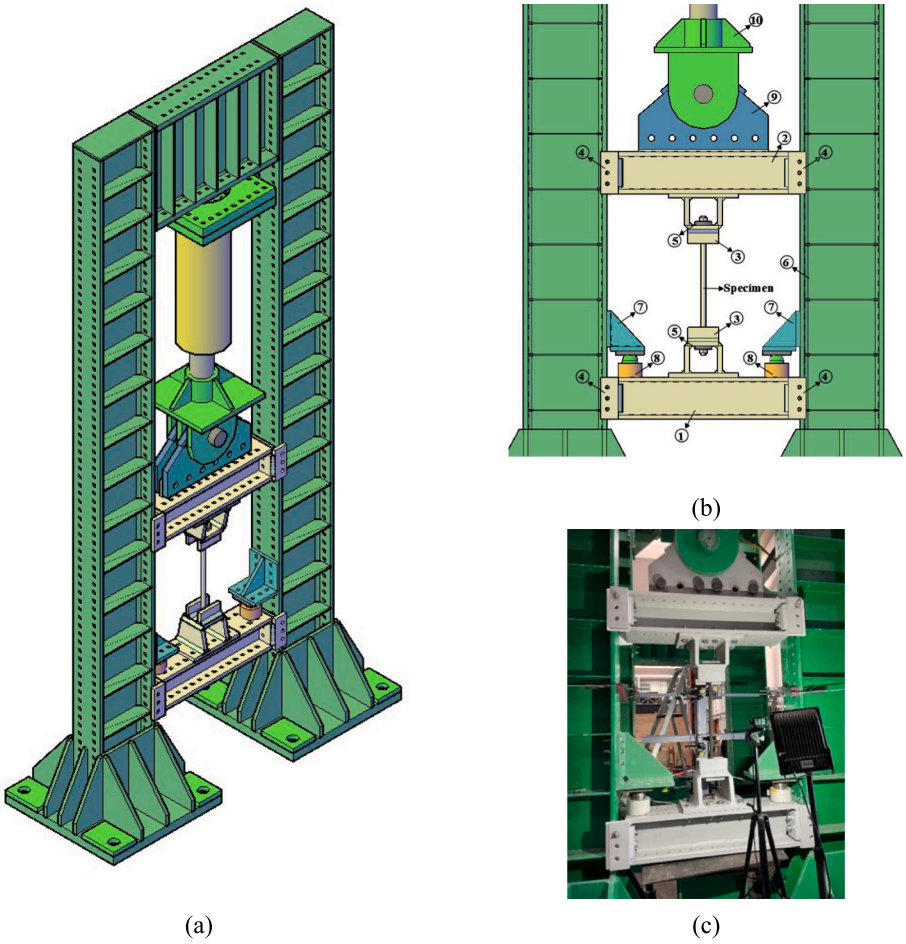

Fig. 6. Test layout: (a) 3D view; (b) Elevation with marked parts; (c) Photo from the test.

Fig. 7. Test layout details: (a) Bolt-to-beam connection tool; (b) Hydraulic jack; (c) Protruding part of the bolt.

A) and relative (label R) displacements of parts of the test. Four of them (A - 1, 2, 3, and 4) were positioned on the top and bottom bolt-to-beam connection tools. These were later used for the calculation of the long bolt elongation. LVDTs A - 5, 6, 7, and 8 were positioned at the edges of the upper retaining beam to assess potential beam rotation during test execution. LVDTs A - 11 and 12 were positioned on the bottom retaining beam, to monitor potential beam bending or rotation. LVDTs R - 9 and 10, measured the relative displacement between the upper and bottom retaining beams and the bolt-to-beam connection tools, thereby detecting any openings between these elements.

3.4. Test results

3.4.1. General

The experimental results comprise the results from the tensile tests of the bolts, following ISO 898-1 [11], clustered according to bolt class and bolt diameter. They are complemented by tensile tests for machined cylindrical steel coupons extracted from the long bolts, according to clause 9.7 of ISO 898-1, and geometrical measurements of the external (d) and internal (d_1) diameters, and pitch length (P).

3.4.2. Geometrical measurements

The real geometrical properties (external and internal diameters, and

Table 4
Nominal geometry and resistance of the bolts.

	Bolt notation		M20	M24	M27	M30
Bolt diameter	d	mm	20	24	27	30
Thread pitch	P	mm	2.5	3.0	3.0	3.5
Tensile area	A_s	mm^2	245	353	459	561
Nut thickness (nominal)	t_n	mm	16	20	22	24
Washer thickness (nominal)	t_w	mm	4	4	5	5
Operational grip length for 1000 mm bolt, single nut N1	$L_{g,N1}$	mm	935	922	916	907
Operational grip length for 1000 mm bolt, double nut N2	$L_{g,N2}$	mm	903	882	872	859
Class 8.8: Design tensile resistance, Eq. (2)	$F_{t,Rd}$	kN	141.1	203.3	264.4	323.1
Class 10.9: Design tensile resistance, Eq. (2)	$F_{t,Rd}$	kN	176.4	254.2	330.5	403.9

pitch length) were measured with a calliper on a sample of long bolt specimens, sorted according to bolt diameter, class and surface finishing. For each group, 3 bolts were measured in 3 different places across their length. Hence, 9 measurements were performed per group, and, in total, 108 measurements for each property. These measurements are summarized in Table 5. An accurate measure of the internal thread diameter was not feasible due to the small thread pitch. Measurements of the thread pitch are based on the length covered by 15 threads l_{15}. The tensile area A_s was calculated using Eq. (1b).

The ratio between as-measured properties and nominal properties is listed in Table 6, showing that the mean value for $A_s/A_{s,nom}$ for black bolts is 0.968 and 0.980 for galvanized bolts. As expected, the ratios are slightly higher for galvanized bolts, due to the coating thickness.

3.4.3. Bolt material tensile tests

Long bolts used in the experimental campaign were made of high-strength steel, classes 8.8 and 10.9, supplied and tested by bolt manufacturer FATOR. Table 7 provides a summary of the coupon tests, totalling 43 coupons.

Material characterization was performed by coupon testing, according to clause 9.7 of ISO 898-1 [11] and ISO 6892-1 [48], providing the full stress-strain curves depicted in Fig. 9.

Table 8 summarizes the results showing mean values per bolt diameter and the mean and coefficient of variation (CoV) across all coupons of the same material. In Table 8, $R_{p,0.2}$, R_m, and R_r are the stress at 0.2 % non-proportional elongation, the tensile strength and the stress at the rapture point, respectively, A_{gt} is the total percentage elongation corresponding to the tensile strength, A is the percentage elongation at fracture. All values satisfy the minimum requirements of ISO 898-1 of $R_{p,0.2,min} \geq 660$ MPa, $R_m \geq 830$ MPa, $A \geq 12$ %, for class 8.8 and $R_{p,min} \geq 940$ MPa, $R_m \geq 1040$ MPa, $A \geq 9$ %, for class 10.9.

3.4.4. Force-displacement curves

The force-displacement curves are presented in Fig. 10. Fig. 10(a) shows the curves for the tests performed with single nuts (N1), whereas Fig. 10(b) shows the equivalent curves for the tests performed with double nuts (N2). In all cases, the maximum load is indicated with the symbol that also corresponds to the failure mode (circle for BF failure, star for TS failure). The different diameters (M20, M24, M27, M30) and the two bolt classes (8.8, 10.9) are labelled in the plots and can be easily distinguished. Bolt finishing surfaces are indicated with full (black) and dashed lines (galvanized).

Adopting the table organization for the test results presented in [32], Table 9 summarizes the test results for the tension tests of the long bolts.

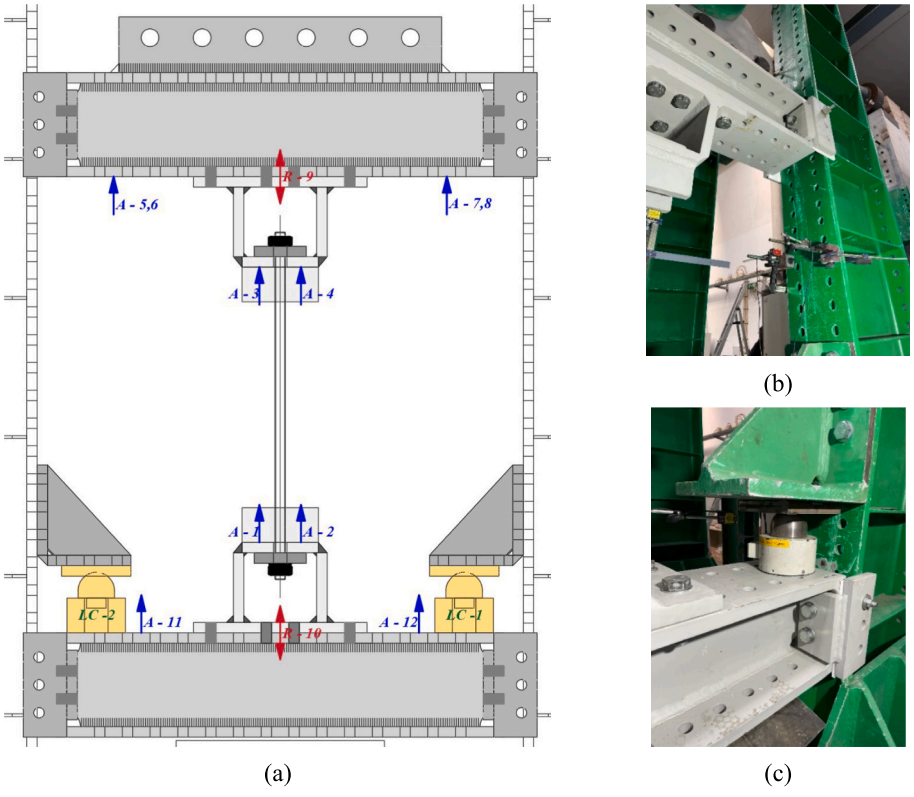

Fig. 8. Instrumentation: (a) Position of the LVDTs and LCs; (b) LVDTs; (c) Load cell.

Table 5
Summary of geometrical characterization.

			Black (B)			Galvanized (G)		
			d (mm)	P (mm)	A_s (mm^2)	d (mm)	P (mm)	A_s (mm^2)
M20	/	Nominal	20.00	2.50	244.79	20.00	2.50	244.79
	8.8	Measured, Mean	19.47	2.53	229.52	19.62	2.53	233.82
		Measured, CoV	0.34 %	0.23 %	0.77 %	0.42 %	0.16 %	0.97 %
		Mean/Nominal	97.34 %	101.17 %	93.76 %	98.12 %	101.06 %	95.52 %
	10.9	Measured, Mean	19.87	2.53	240.47	19.98	2.53	243.54
		Measured, CoV	0.12 %	0.33 %	0.28 %	0.07 %	0.14 %	0.17 %
		Mean/Nominal	99.34 %	101.04 %	98.23 %	99.90 %	101.08 %	99.49 %
M24	/	Nominal	24.00	3.00	352.50	24.00	3.00	352.50
	8.8	Measured, Mean	23.79	3.02	344.84	23.87	3.01	347.75
		Measured, CoV	0.38 %	0.21 %	0.91 %	0.16 %	0.20 %	0.39 %
		Mean/Nominal	99.12 %	100.74 %	97.82 %	99.45 %	100.43 %	98.65 %
	10.9	Measured, Mean	23.72	3.03	342.34	23.84	3.03	346.48
		Measured, CoV	0.15 %	0.18 %	0.34 %	0.15 %	0.10 %	0.33 %
		Mean/Nominal	98.84 %	101.07 %	97.12 %	99.35 %	100.93 %	98.29 %
M27	/	Nominal	27.00	3.00	459.41	27.00	3.00	459.41
	10.9	Measured, Mean	26.54	3.02	441.27	26.69	3.02	446.93
		Measured, CoV	0.27 %	0.24 %	0.60 %	0.34 %	0.16 %	0.76 %
		Mean/Nom	98.30 %	100.83 %	96.05 %	98.84 %	100.62 %	97.28 %
M30	/	Mean/Nominal	30.00	3.50	560.59	30.00	3.50	560.59
	10.9	Measured, Mean	29.75	3.51	549.82	29.86	3.51	554.44
		Measured, CoV	0.11 %	0.15 %	0.26 %	0.24 %	0.16 %	0.55 %
		Mean/Nom	99.18 %	100.38 %	98.08 %	99.54 %	100.24 %	98.90 %
All	/	Max CoV	0.38 %	0.33 %	**0.91 %**	0.42 %	0.20 %	**0.97 %**

Table 6
Comparison of as-measured and nominal geometrical properties.

	Black (B)			Galvanized (G)			Total		
	d/d_{nom} (−)	P/P_{nom} (−)	$A_s/A_{s,nom}$ (−)	d/d_{nom} (−)	P/P_{nom} (−)	$A_s/A_{s,nom}$ (−)	d/d_{nom} (−)	P/P_{nom} (−)	$A_s/A_{s,nom}$ (−)
Mean	0.987	1.009	0.968	0.992	1.007	0.980	0.989	1.008	0.974
CoV	0.74 %	0.35 %	1.72 %	0.63 %	0.35 %	1.45 %	0.74 %	0.35 %	1.69 %
Max	0.995	1.014	0.988	1.000	1.014	0.997	1.000	1.014	0.997
Min	0.969	1.001	0.927	0.975	1.000	0.941	0.969	1.000	0.927

Table 7
Summary of coupon tests.

Class	Bolt	No. of batches	No. of coupons
8.8	M20	2	6
	M24	2	6
	M27	1	4
	M30	1	4
10.9	M20	2	6
	M24	2	6
	M27	2	6
	M30	2	5
		Total:	43

The following observations can be derived from Fig. 10 and Table 9:

- M20 8.8 bolts present a marked yield plateau, that is not apparent for all other bolts.
- The plots confirm that all tests with double nut failed by Bolt Fracture (BF), and a large proportion of tests with single nut (N1) failed by Thread Stripping TS. In addition, tests failing by BF achieved larger ductility than those with TS failure and featured more consistent values of maximum force and corresponding displacement.
- Tests failing by TS present a large scatter in terms of maximum force and corresponding displacement; about 50 % of the failures by TS for 10.9 bolts occur prior to bolt yielding.

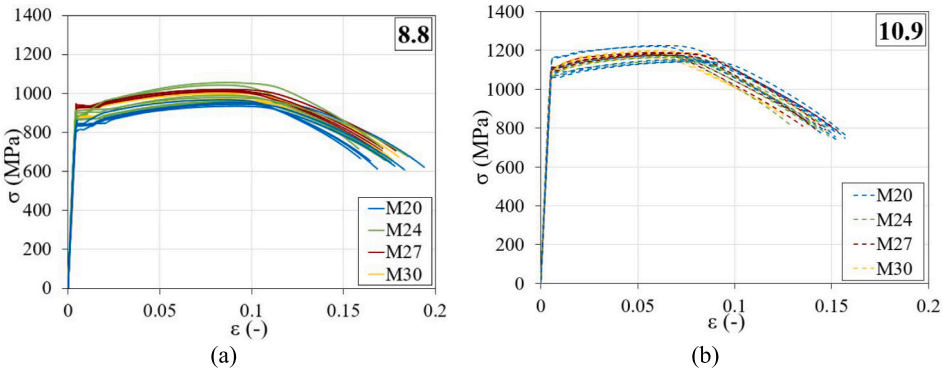

Fig. 9. Stress-strain curves for long bolts: (a) Class 8.8; (b) Class 10.9.

Table 8
Bolt coupon test results from machined test pieces.

Class	Bolt		$R_{p,0.2} = f_y$ (MPa)	$R_m = f_{ub}$ (MPa)	R_r (MPa)	A_{gt} (%)	A (%)
	M20	Mean	833.6	950.6	630.4	9.13	17.15
	M24	Mean	883.2	995.9	683.9	8.53	16.88
	M27	Mean	930.3	1013.7	705.6	8.29	16.87
8.8	M30	Mean	895.9	984.7	672.1	8.13	17.28
		Mean	880.3	983.6	669.8	8.58	17.04
	Total	Mean/Nominal	1.38	1.23	–	–	1.42
		CoV	4.32 %	3.45 %	5.27 %	5.63 %	5.00 %
	M20	Mean	1109.4	1176.1	754.8	6.86	14.93
	M24	Mean	1083.8	1166.6	797.9	6.47	13.73
	M27	Mean	1107.0	1183.3	800.6	6.42	14.05
10.9	M30	Mean	1104.3	1187.0	859.6	6.08	12.77
		Mean	1101.0	1177.9	800.8	6.48	13.92
	Total	Mean/Nominal	1.22	1.18	–	–	1.55
		CoV	2.29 %	1.83 %	5.12 %	10.00 %	7.09 %

- For tests failing by BF, 8.8 bolts present higher ductility than 10.9 bolts.

For bolts failing by BF, it is observed that the descending part of the curve after the maximum load is significantly shorter compared to the standard structural bolts tested in the literature. This was due to the test layout, because the bottom beam (see (1) in Fig. 6), and its fittings were hanging from the long bolt. Although this effect was not relevant until the maximum load was reached (its self-weight of about 500 kg was deducted from the load cell measurements), it affected the behaviour after reaching this point, transforming the test from pure displacement control into a hybrid displacement/force control test, thereby preventing the capture of the descending equilibrium path.

To demonstrate this, four additional tests were conducted using a standard universal tensile testing machine with a 600 kN capacity (see Fig. 11), following strictly the prescribed test specifications of ISO 898-1 [11]. It is noted that the total bolt length had to be reduced to 400 mm because of equipment limitations. To ensure BF failure mode, double nuts were used at each end. The test conditions remained consistent with the prior experiments, utilizing bolts from the same batches as in the previous tests and a loading speed of 0.025 mm/s.

Fig. 12 compares the load-displacement behaviour of the additional tests with the corresponding tests described in Table 9 (T4, T16, T25 and T37) and two reference tests from the literature (Stranghöner et al. [32]) on standard structural bolts. Normalized displacement and force values are used on the x- and y-axis, given that 3 different bolt diameters are compared (Stranghöner et al.'s tests were conducted on M16 bolts, whereas the tests carried out in the present study correspond to M20 and M24 long bolts).

Comparing tests T4, T16, T25, and T37 with additional tests AT1 to AT4, much larger ductility ratios and ratios of elongation at fracture versus elongation at maximum load are observed for the latter tests. For bolt class 8.8, similar ductility is observed between tests AT1 and AT2 and Stranghöner et al.'s test, while for bolt class 10.9, tests AT3 and AT4 exhibit about 50 % less ductility when compared to Stranghöner et al.'s test.

Table 10 compares the experimentally measured initial stiffness with the results from Eq. (3). A good match is obtained but a trend of decreasing measured stiffness with increasing bolt diameter is observed ($0.915 < 0.997 < 1.015 < 1.065$). Additionally, comparing the use of one nut against two nuts, smaller initial stiffness is observed for double nuts, probably reflecting the assumption of measuring the bolt elongation length from the midpoint of the two nuts.

3.4.5. *Failure modes*

The same failure modes for this type of load, as previously

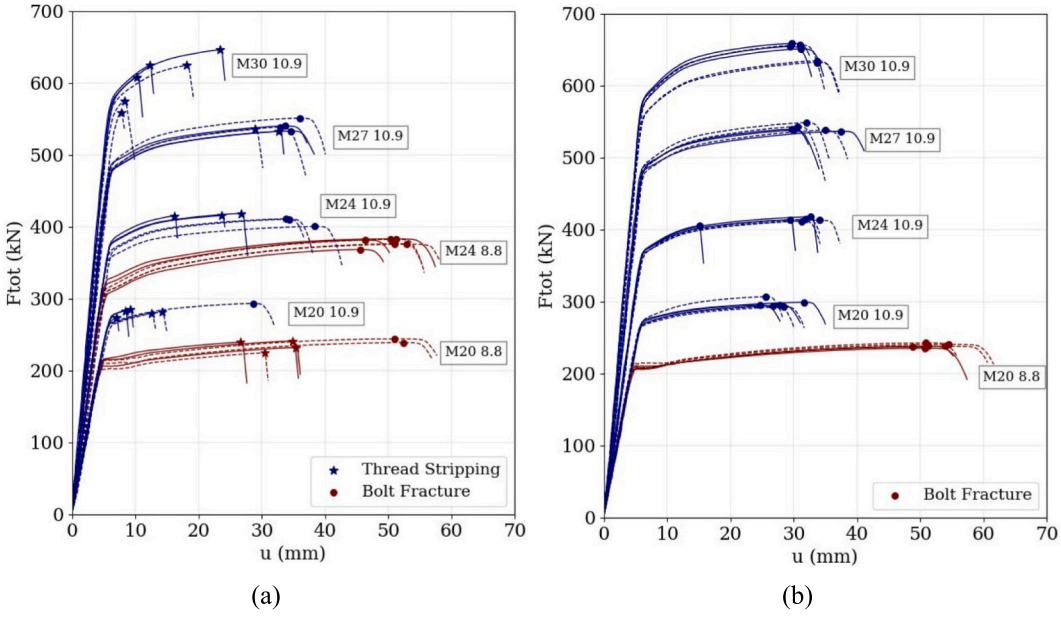

Fig. 10. Force-displacement curves: (a) Tests with single nut (N1); (b) Tests with double nut (N2).

Table 9
Summary of the results of tensile tests of the long bolts.

Bolt	Class	No. of nuts	No. of tests	Test labels	Mean tensile stress area $A_{s,\ meas,mean}$ (mm^2)	Max. tensile load $F_{mf,\ exp,\ mean}$ (kN)	Tensile strength $R_{mf,mean} = f_{ub,exp,\ mean}$ (MPa)	CoV ($R_{mf,\ mean}$)	Over-strength ratio $f_{ub,exp,\ mean}/f_{ub,nom}$ (MPa)	Calculated tension resistance of the long bolt $F_{mf,calc,mean}$ (kN)	Load at 0.0048d non-proportional elongation $F_{pf,\ exp.\ mean}$ (kN)	$R_{pf,exp,mean} = f_{yb,\ exp,mean}$ (MPa)	Yield strength CoV ($R_{pf,exp,\ mean}$)	Elong-ation after fracture $A_{f,\ exp,\ mean}$ (−)	Failure mode	
															TS	BF
M20	8.8	1	6	T1-T3, T7-T9	231.7	237.0	953.1	0.06 %	1.19	220.8	207.9	841.0	0.61 %	1.39	67 %	33 %
		2	6	T4-T6, T10-T12	231.7	238.8	953.1	0.06 %	1.19	220.8	204.1	841.0	0.61 %	1.94	0 %	100 %
	10.9	1	6	T13-T15, T19–12	242.0	283.8	1188.6	4.35 %	1.19	287.7	254.4	1125.1	4.49 %	0.31	83 %	17 %
		2	6	T16-T18, T22-T24	242.0	297.2	1188.6	4.35 %	1.19	287.7	260.9	1125.1	4.49 %	0.88	0 %	100 %
M24	8.8	1	6	T25-T30	346.3	378.1	1048.2	0.85 %	1.31	363.0	309.1	881.4	0.48 %	1.52	0 %	100 %
	10.9	1	6	T31-T36	344.4	414.5	1159.0	1.44 %	1.16	399.2	373.2	1079.3	1.61 %	0.61	100 %	0 %
		2	6	T37-T42	344.4	410.3	1159.0	1.44 %	1.16	399.2	349.6	1079.3	1.61 %	0.96	0 %	100 %
M27	10.9	1	6	T43-T45, T49-T51	444.1	538.9	1180.3	0.56 %	1.18	524.2	470.5	1103.8	1.05 %	0.82	33 %	67 %
		2	6	T46-T48, T52-T54	444.1	540.8	1180.3	0.56 %	1.18	524.2	464.9	1103.8	1.05 %	0.80	0 %	100 %
M30	10.9	1	6	T55-T57, T61-T63	552.1	606.2	1187.4	–	1.19	655.6	554.1	1107.2	–	0.19	100 %	0 %
		2	6	T58-T60, T64-Y66	552.1	648.0	1187.4	–	1.19	655.6	552.1	1107.2	–	0.69	0 %	100 %

Fig. 11. Layout of the additional tensile test of the cut long bolt.

documented in the literature for the conventional bolts [30], were observed in this study. The two observed failure modes were: (i) thread stripping (TS), see Fig. 13(a); and (ii) bolt fracture (BF), see Fig. 13(b).

From Fig. 10 the following trends can be established:

- For all tests where double nuts were used (N2), failure occurred by BF.
- When only a single nut was used (N1), 64 % of all tests resulted in TS failure, while 36 % resulted in BF failure.
- For 10.9 bolts, the proportion of cases failing by TS is larger than for 8.8 bolts.
- All M24 10.9 and M30 10.9 bolts with single nut (N1) failed by TS.
- All M24 8.8 bolts with single nut (N1) failed by BF.

As a summary for practical application, if BF failure is desired for long bolts subjected to tension, the use of a double nut (N2) is recommended.

4. Stress-strain curves for bolt material

The use of advanced numerical simulations with sophisticated finite element models whereby the bolts are modelled with solid elements is becoming increasingly common [39,43], further enhanced by a new part of Eurocode 3 dedicated to design by finite elements. FprEN 1993–1-14 [49] provides stress-strain models for structural steels but it currently lacks guidance for the stress-strain curves of structural bolts.

Recently, Yang et al. [50] proposed a material stress-strain model for the steel material of high-strength steel bolts that includes the effect of strain rate, based on the Yun and Gardner model [51], reproduced in Eqs. (4) to (7) for the case of no strain rate.

$$\sigma = \begin{cases} E\varepsilon & \text{for} \quad \varepsilon \le \varepsilon_y \\ f_y & \text{for} \quad \varepsilon_y < \varepsilon \le \varepsilon_{sh} \\ f_y + \left(f_u - f_y\right)\left[0.4\varepsilon^* + \dfrac{2\varepsilon^*}{\left(1+400\varepsilon^{*5}\right)^{0.2}}\right] & \text{for} \quad \varepsilon_{sh} < \varepsilon \le \varepsilon_u \end{cases} \tag{4}$$

where

$$\varepsilon^* = \frac{\varepsilon - \varepsilon_{sh}}{\varepsilon_u - \varepsilon_{sh}} \tag{5}$$

$$\varepsilon_{sh} = \begin{cases} 0.0163 & \text{for} \quad \text{class 8.8 bolts} \\ 0 & \text{for} \quad \text{class 12.9 bolts} \end{cases} \tag{6}$$

$$\varepsilon_u = 0.6\left(1 - \frac{f_y}{f_u}\right), \text{but } \varepsilon_u \ge 0.06. \tag{7}$$

It is noted that Yang et al. [50] identify a steel plateau for class 8.8 bolts and no plateau for class 12.9, whereby no information is provided for class 10.9. It is also noted that the original proposal by Yun and

Table 10
Comparison of experimental and code results for initial stiffness.

Bolt	Class	No. of nuts	No. of tests	$k_{b,nom}$ / $k_{b,exp}$	
				Mean	CoV
M20	8.8	1	6	0.87	2.85 %
		2	6	0.91	3.78 %
	10.9	1	6	0.92	5.78 %
		2	6	0.96	2.61 %
M24	8.8	1	6	0.98	5.16 %
	10.9	1	6	0.96	6.88 %
		2	6	1.05	3.59 %
M27	10.9	1	6	0.98	4.93 %
		2	6	1.05	3.94 %
M30	10.9	1	6	1.03	4.52 %
		2	6	1.10	3.48 %
ALL			**66**	**0.98**	**7.93 %**

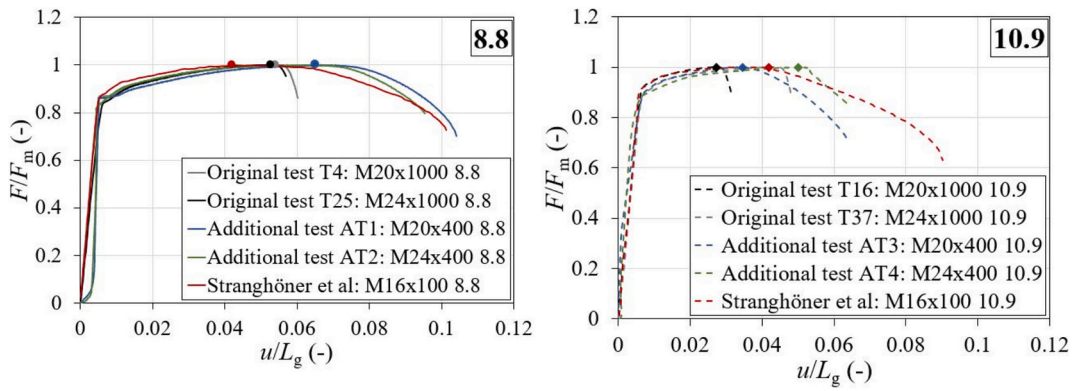

Fig. 12. Comparative force-displacement results.

Fig. 13. Failure modes: (a) Thread stripping; (b) Bolt fracture.

Table 11
Engineering strains for bolt coupon test results from machined test pieces.

		ε_y	ε_{sh}	$\varepsilon_{sh}/\varepsilon_y$	ε_u	$\varepsilon_u/\varepsilon_y$
8.8	Mean	0.00430	0.01395	3.25	0.0858	19.97
	CoV	5.4 %	36.5 %	–	5.6 %	–
10.9	Mean	0.00531	0.00893	1.68	0.0648	12.20
	CoV	5.1 %	24.4 %	–	10.0 %	–

Gardner for hot-rolled steel for the strain hardening strain ε_{sh} is given by Eq. (8) as:

$$\varepsilon_{sh} = 0.1\frac{f_y}{f_u} - 0.055, \text{ but } 0.015 \leq \varepsilon_{sh} \leq 0.03 \quad (8)$$

Table 11 summarizes the results from the experimental coupon tests for ε_y, ε_{sh} and ε_u for 8.8 and 10.9 bolt materials. Comparison with the results by Yang et al. [50] for 8.8 bolt material shows a slightly higher value for ε_{sh} (17 %: 0.0163 vs 0.01395), and a significantly higher value for ε_u (40 %: 0.12 vs 0.0858). However, the coupon test results for M20 and M24 bolt material exhibit an unusually high scatter for ε_{sh}, so an average value of $\varepsilon_{sh} = 0.015$ is adopted. Concerning ε_u, Yang et al.'s model simply adopted Eq. (8) from the Yun and Gardner model, so that a value of $\varepsilon_u = 0.086$ is adopted.

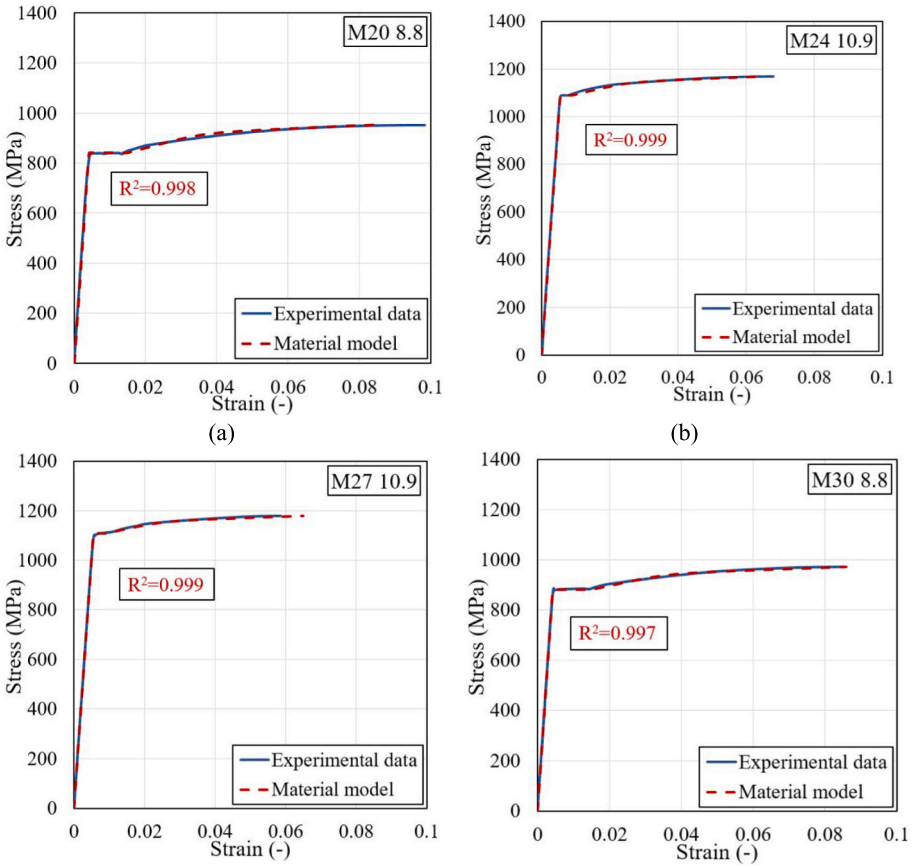

Fig. 14. Application of the proposed model to selected coupons: a) M20 8.8; b) M24 10.9; c) M27 10.9; d) M30 8.8.

Table 12
Assessment of the proposed model: summary of R^2 values.

		8.8	10.9	ALL
Stress-strain curve	Mean	0.993	0.998	0.996
	CoV	0.77 %	0.10 %	0.41 %
ε_{sh}	Mean	0.993	0.998	0.996
ε_u	Mean	0.996	0.998	0.997

Hence, it is proposed to adopt the Yun and Gardner model for bolt material classes 8.8 and 10.9 (Eqs. (4) and (5)), with Eqs. (6) and (7) replaced as follows:

$$\varepsilon_{sh} = \begin{cases} 0.015 & \text{for class 8.8 bolts} \\ 0.0089 & \text{for class 10.9 bolts} \end{cases} \quad (9)$$

$$\varepsilon_u = \begin{cases} 0.086 & \text{for class 8.8 bolts} \\ 0.065 & \text{for class 10.9 bolts} \end{cases} \quad (10)$$

For all tests, the experimental curves were compared to the material model. Fig. 14 illustrates its application to a few selected examples, showing good agreement.

Table 12 shows the results of the application of the proposed model to the tests. The comparison yields an average R^2 value of 0.996 for the full-stress-strain curve across all tests, indicating excellent agreement. The bottom two rows of the Table 12 present the R^2 values calculated for ε_{sh} or ε_u (Eqs. (9) and (10)), showing similar results.

5. Reliability assessment

5.1. Methodology

The statistical evaluation is carried out by following the methodology described in the EN 1990, Annex D [9] and the detailed procedures presented in the SAFEBRICTILE project [52]. Considering the split between loading and resistance [53], the target reliability index to be considered for reliability class RC2 is $\beta = 3.04$. The reliability assessment comprises the following steps: (i) statistical characterization of the basic variables; (ii) determination of the variability of the design method; (iii) calculation of the required partial factor γ_{M2}* that satisfies the target reliability index.

5.2. Statistical characterization of the basic variables

According to Eq. (2), the basic variables for the reliability assessment of the tensile strength of steel bolts are the tensile strength f_{ub} and the tensile stress area A_s. Their statistical characterization is addressed in the following subsections.

5.2.1. Tensile strength

Test results reported in Table 8 show an average ratio $f_{ub,exp,mean}/f_{ub,nom} = 1.23$ and a coefficient of variation $CoV(f_{ub,exp}) = 3.45$ % for class 8.8 and $f_{ub,exp,mean}/f_{ub,nom} = 1.18$ and a coefficient of variation $CoV(f_{ub,exp}) = 1.83$ % for class 10.9. This agrees well with the coefficient of variation conservatively adopted by Stranghöner et al. [32] of 4 % which is also adopted here for consistency with that study.

5.2.2. Cross-sectional area

The measurements reported in Table 5 show that the maximum coefficients of variation for d, P and A_s are, respectively, 0.42 %, 0.33 % and 0.97 %. The latter is in line with the 1 % $CoV(A_s)$ value adopted by Stranghöner et al. [32], which is also adopted here for consistency with that study. The ratio between the measured tensile area and the nominal tensile area, $A_{s,meas,mean}/A_{s,nom}$, shown in Table 6, is 0.974.

5.3. Tension resistance

The experimental results are first compared to the theoretical results obtained by Eq. (2) with $\gamma_{M2} = 1.0$, and measured material properties in Fig. 15. Fig. 15(a) compares the experimental resistance using $k_2 = 0.9$, as specified in EN 1993–1-8 [6], while Fig. 15(b) adopts $k_2 = 1.0$ as proposed by Stranghöner et al. [32]. Table 13 reports on the corresponding required partial factor γ^*_{M2} for both cases, showing results that are slightly higher than those obtained by Stranghöner et al. for standard structural bolts. However, it is noted that the results by Stranghöner et al. correspond to a mix of property classes 4.6, 5.6, 8.8 and 10.9.

Since the recommended value of γ_{M2} in EN 1993–1-8 [6] is 1.25, the results of Table 13 may support increasing k_2 from 0.9 to 1.0, as also proposed by Stranghöner et al. However, there are additional aspects that need to be considered:

- EN 1990 [9] does not address the issue of reliability differentiation as a function of the nature of the failure mode [54]. Nevertheless, historically, since the ENV versions of Eurocode 3, the adoption of the partial factors γ_{M0}, γ_{M1} and γ_{M2} always implicitly incorporated

Table 13
Reliability assessment of the required partial factor γ^*_{M2}.

k_2	b	V_δ	γ^*_{M2}	γ^*_{M2} [32]
0.90	**1.116**	0.054	**0.955**	0.88
1.00	1.004		1.061	0.98

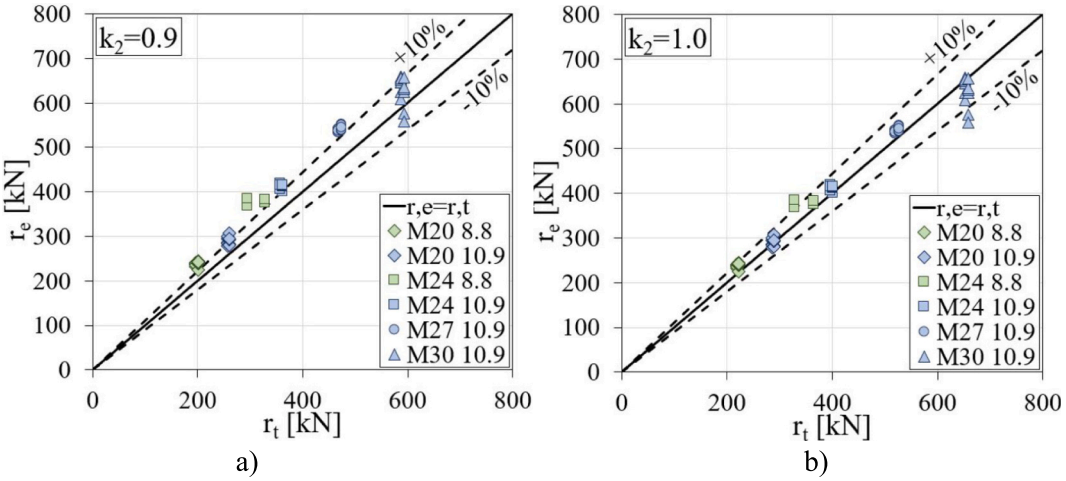

Fig. 15. Comparison of theoretical and experimental tension resistance for long bolts: a) $k_2 = 0.9$; b) $k_2 = 1.0$.

reliability differentiation in an empirical way by establishing $\gamma_{M2} = 1.25$ for failure modes driven by fracture and $\gamma_{M0} = 1.0$ for failure modes driven by plasticity. For example, the reliability assessment of the newly introduced expressions for the design resistance of butt and fillet welds clearly showed that $\gamma^{*}_{M2} \leq 1.05$ [55], but the adopted partial factor was kept as 1.25.

- Secondly, Eq. (2) provides the design tension resistance for the verification of bolts in, e.g., bolted endplate joints, whereby the T-Stub model is used. However, in the case of a Mode 2 failure mode, the bolts present second-order bending deformations that are not covered by Eq. (2).

6. Conclusions

This paper presents a comprehensive experimental campaign on long bolts in tension, with the variability of relevant parameters including bolt diameter, bolt class, number of nuts and finishing surfaces. In total 66 tests were conducted. The following conclusions can be derived:

- The observed failure modes were in correspondence with the previous tests found in the literature for standard structural bolts. Bolt fracture failure (BF) occurred in all tests with double nuts (N2), whereas in tests with single nuts (N1), a large proportion of cases (64 %) failed by thread stripping (TS).
- The existing analytical formulas for the design tensile resistance of standard structural bolts provided by EN 1993–1-8 can be safely applied to long bolts.
- The expression for initial stiffness provides a good approximation to the measured values, exhibiting a trend of decreasing stiffness with increasing bolt diameter.
- Class 8.8 long bolts showed similar levels of ductility when compared to equivalent standard structural bolts, while for class 10.9 long bolts a reduction of about 50 % was noted when compared to Stranghöner et al.'s tests.

Finally, although the results show that it is possible to increase the tension resistance of bolts by adopting $k_2 = 1.0$ while maintaining the target reliability of $\beta = 3.04$, it is believed that a wider discussion needs to be undertaken concerning reliability differentiation and bending effects in bolts in moment-resisting joints.

Acknowledgment and funding sources

This work was partly financed by:

- The European Commission's Research Fund for Coal and Steel through the research project CONNECT4C (High-strength steel connections for circular construction), ref. no. 101112300, is highly acknowledged. Disclaimer: "Work is funded by Europe Union. Views and opinions expressed are however those of the author(s) only and do not necessarily reflect those of the European Union or European Research Executive Agency (REA). Neither the European Union nor the granting authority can be held responsible for them."
- FCT / MCTES through national funds (PIDDAC) under the R&D Unit Institute for Sustainability and Innovation in Structural Engineering (ISISE), under reference UIDB / 04029/2020 (https://doi.org/10.54499/UIDB/04029/2020), and the Associate Laboratory Advanced Production and Intelligent Systems (ARISE) under reference LA/P/0112/2020.

CRediT authorship contribution statement

Neda Janković: Writing – review & editing, Writing – original draft, Validation, Software, Methodology, Investigation. **Filip Ljubinković:** Writing – original draft, Validation, Supervision, Methodology, Conceptualization. **Jorge Conde:** Writing – review & editing, Writing – original draft, Validation, Supervision, Software, Methodology, Formal analysis, Conceptualization. **Jordi Costa:** Writing – review & editing, Methodology. **Luís Simões da Silva:** Writing – review & editing, Writing – original draft, Validation, Supervision, Software, Methodology, Formal analysis, Conceptualization.

Declaration of competing interest

The authors declare that they have no known competing financial interests or personal relationships that could have appeared to influence the work reported in this paper.

Data availability

Data will be made available on request.

References

[1] E. Elettore, F. Freddi, M. Latour, G. Rizzano, Parametric study and finite element analysis of self-centring steel column bases with different structural properties, J. Constr. Steel Res. 199 (2022) 107628.
[2] A. Lettieri, A. de la Peña, F. Freddi, M. Latour, Damage-free self-centring links for eccentrically braced frames: development and numerical study, J. Constr. Steel Res. 201 (2023) 107727.
[3] H. Van-Long, J. Jean-Pierre, D. Jean-François, Extended end-plate to concrete-filled rectangular column joint using long bolts, J. Constr. Steel Res. 113 (2015) 156–168.
[4] European Committee for Standardization, EN 15048–1:2007: Non-preloaded Structural Bolting Assemblies – Part 1: General Requirements, 2007. Brussels, Belgium.
[5] European Committee for Standardization, EN 14399–4:2015: High-Strength Structural Bolting Assemblies for Preloading – Part 4: System HV – Hexagon Bolt and Nut Assemblies, 2015. Brussels, Belgium.
[6] European Committee for Standardization, EN 1993–1-8:2005: Eurocode 3: Design of Steel Structures - Part 1–8: Design of Joints, 2005. Brussels, Belgium.
[7] L. Simões da Silva, F. Ljubinković, J. Conde, T. Alves, J.F. Demonceau, A. Neutelers, C. Odenbreit, T. Bogdan, K. Mela, A. Bernabeu, G. González, CONNECT4C: High-strength steel connections for circular construction, in: RFCS-02-2022-RPJ, Deliverable D1.1 – Comprehensive Overview of the Project, 2023.
[8] N. Janković, J. Dobrić, N. Gluhović, J. Conde, F. Ljubinković, L.S. da Silva, Numerical characterization of innovative demountable beam-column connections using long, ce/papers 7 (1–2) (2024) 45–54.
[9] European Committee for Standardization, EN 1990:2002: Eurocode – Basis of Structural Design, 2002. Brussels, Belgium.
[10] European Committee for Standardization, EN 14399–1:2015: High-Strength Structural Bolting Assemblies for Preloading - Part 1: General Requirements, 2015. Brussels, Belgium.
[11] European Committee for Standardization, ISO 898-1:2013: Mechanical Properties of Fasteners Made of Carbon Steel and Alloy Steel - Part 1: Bolts, Screws and Studs with Specified Property Classes - Coarse Thread and Fine Pitch Thread, 2013. Brussels, Belgium.
[12] European Committee for Standardization, ISO 261:1998: General Purpose Metric Screw Threads - General Plan, 1998.
[13] European Committee for Standardization, ISO 724:1993: General Purpose Metric Screw Threads – Basic Dimensions, 1993.
[14] European Committee for Standardization, ISO 888:2012: Fasteners - Bolts, Screws and Studs - Nominal Lengths and Thread Lengths, 2012.
[15] European Committee for Standardization, ISO 3508:1976: Thread Run-outs for Fasteners with Thread in accordance with IS0 261 and IS0 262, 1976.
[16] European Committee for Standardization, ISO 4014:2011: Hexagon Head Bolts – Product Grades A and B, 2011.
[17] European Committee for Standardization, ISO 4017:2022: Fasteners - Hexagon Head Screws - Product Grades A and B, 2022.
[18] European Committee for Standardization, ISO 4753:2011: Fasteners - Ends of Parts with External ISO Metric Thread, 2011.
[19] European Committee for Standardization, ISO 965-1:1998: ISO General Purpose Metric Screw Threads - Tolerances - Part 1: Principles and Basic Data, 1998.
[20] European Committee for Standardization, ISO 4759-1:2000: Tolerances for Fasteners - Part 1: Bolts, Screws, Studs and Nuts - Product Grades A, B and C, 2000.
[21] European Committee for Standardization, ISO 4042:2018: Fasteners - Electroplated Coating Systems, 2018.
[22] European Committee for Standardization, ISO 6157-1:1988: Fasteners – Surface Discontinuities - Part 1: Bolts, Screws and Studs for General Requirements, 1988.
[23] European Committee for Standardization, ISO 10683:2018: Fasteners – Non-Electrolytically Applied Zinc Flake Coating Systems, 2018.
[24] European Committee for Standardization, EN 15048–2:2016: Non-preloaded Structural Bolting Assemblies - Part 2: Fitness for Purpose, 2016.
[25] European Committee for Standardization, ISO 3269:2019: Fasteners -Acceptance Inspection, 2019.

[26] European Committee for Standardization, EN 14399–2:2015: High-strength Structural Bolting Assemblies for Preloading - Part 2: Suitability for Preloading, 2015.
[27] I. Lourenço, Mobile Applications: Design of Connections (in Portuguese), MSc thesis, University of Coimbra, 2013.
[28] European Committee for Standardization, EN 14399–3:2015: High-strength Structural Bolting Assemblies for Preloading - Part 3: System HR - Hexagon Bolt and Nut Assemblies, 2015.
[29] M. D'Aniello, D. Cassiano, R. Landolfo, Monotonic and cyclic inelastic tensile response of European preloadable gr10.9 bolt assemblies, J. Constr. Steel Res. 124 (2016) 77–90.
[30] E.L. Grimsmo, A. Aalberg, M. Langseth, A.H. Clausen, Failure modes of bolt and nut assemblies under tensile loading, J. Constr. Steel Res. 126 (2016) 15–25.
[31] European Committee for Standardization, ISO 68-1:1998: ISO General Purpose Screw Threads - Basic Profile - Part 1: Metric Screw Threads, 1998.
[32] N. Stranghöner, C. Abraham, L. Ehrhardt, New design approaches for tension, shear and interaction resistance of carbon steel bolts, J. Constr. Steel Res. 212 (2024) 108260.
[33] G.L. Kulak, J.W. Fisher, J.H. Struik, Guide to Design Criteria for Bolted and Riveted Joints Second Edition, 2001.
[34] European Committee for Standardization, ISO 4033:2012: Hexagon High Nuts, 2012. Brussels, Belgium.
[35] E.M. Alexander, Analysis and design of threaded assemblies, SAE Trans. (1977) 1838–1852.
[36] R. Tartaglia, M. D'Aniello, M. Zimbru, Experimental and numerical study on the T-stub behaviour with preloaded bolts under large deformations, Structures 27 (2020) 2137–2155.
[37] E.L. Grimsmo, A.H. Clausen, M. Langseth, A. Aalberg, An experimental study of static and dynamic behaviour of bolted end-plate joints of steel, Int. J. Impact Eng. 85 (2015) 132–145.
[38] F. Yang, M. Veljkovic, Y. Liu, Fracture simulation of partially threaded bolts under tensile loading, Eng. Struct. 226 (2021) 111373.
[39] Y. Hu, L. Shen, S. Nie, B. Yang, W. Sha, FE simulation and experimental tests of high-strength structural bolts under tension, J. Constr. Steel Res. 126 (2016) 174–186.
[40] G. Zhou, Y. An, Z. Wu, D. Li, J. Ou, Analytical model for initial rotational stiffness of steel beam to concrete-filled steel tube column connections with bidirectional bolts, J. Struct. Eng. 144 (11) (2018) 04018199.
[41] L.Y. Wu, L.L. Chung, S.F. Tsai, T.J. Shen, G.L. Huang, Seismic behavior of bolted beam-to-column connections for concrete filled steel tube, J. Constr. Steel Res. 61 (10) (2005) 1387–1410.
[42] H. Fransplass, M. Langseth, O.S. Hopperstad, Tensile behaviour of threaded steel fasteners at elevated rates of strain, Int. J. Mech. Sci. 53 (11) (2011) 946–957.
[43] H. Fransplass, M. Langseth, O.S. Hopperstad, Numerical study of the tensile behaviour of threaded steel fasteners at elevated rates of strain, Int. J. Impact Eng. 54 (2013) 19–30.
[44] H. Fransplass, M. Langseth, O.S. Hopperstad, Tensile behaviour of threaded steel fasteners at elevated rates of strain, Int. J. Mech. Sci. 53 (11) (2011) 946–957.
[45] A. Loureiro, M. López, R. Gutiérrez, J.M. Reinosa, Experimental comparison between threaded-bars and single-bolts end plate asymmetrical steel joints, ce/papers 6 (3–4) (2023) 1185–1189.
[46] American national standard, AISC 360–22: Specification for Structural Steel Buildings, 2022.
[47] Australian standard, AS4100:2020: Steel Structures, 2020.
[48] European Committee for Standardization, ISO 6892-1:2019: Metallic Materials - Tensile Testing - Part 1: Method of Test at Room Temperature, 2019.
[49] European Committee for Standardization, FprEN 1993–1-14: Eurocode 3: Design of Steel Structures - Part 1–14: Design Assisted by Finite Element Analysis, 2025. Brussels, Belgium.
[50] S. Yang, Y. Zhu, R. Zhang, Y. Zhao, H. Yang, Rate-dependent behaviour of high-strength steel bolts, J. Constr. Steel Res. 215 (2024) 108560.
[51] X. Yun, L. Gardner, Stress-strain curves for hot-rolled steels, J. Constr. Steel Res. 133 (2017) 36–46.
[52] L. Simões da Silva, L. Marques, T. Tankova, C. Rebelo, U. Kuhlmann, A. Kleiner, J. Spiegler, H.H. Snijder, R. Dekker, V. Dehan, C. Haremza, A. Taras, L.G. Cajot, O. Vassart, N. Popa, SAFEBRICTILE: Standardization of Safety Assessment Procedures across Brittle to Ductile Failure Modes, 2017 (RFSR-CT-2013-00023, Final Report), 2017.
[53] H. Gulvanessian, J.-A. Calgaro, M. Holicky, Designer's Guide to EN 1990: Eurocode: Basis of Structural Design, Thomas Telford, 2002.
[54] T. Vrouwenvelder, S. Dimova, M.L. Sousa, J. Marková, G. Mancini, U. Kuhlmann, A. Taras, R. Jockwer, W. Jäger, T. Schweckendiek, P. Franchin, D. Skejić, J. D. Sørensen, P. Spehl, M. Stacy, M. Feldmann, P. Croce, B. Zhao, P. Tanner, J. Knippers, M. Mollaert, J. André, R. Steenbergen, J. Kohler, T. Bakeer, J. Maljaars, D. Allaix, J. Spross, Reliability Background in the Eurocodes - Support to the Implementation, Harmonization and Further Development of the Eurocodes (EUR 40072). https://data.europa.eu/doi/10.2760/9482837, 2024.
[55] J. Spiegler, Load Capacity from Fillet Weld and Butt Weld Joints of High-Strength Structural Steels, PhD thesis, University of Stuttgart, 2022.